Properties of Resonantly Heated Electron Distributions

Kent Estabrook and W. L. Kruer
University of California, Lawrence Livermore Laboratory, Livermore, California 94550
(Received 24 June 1977)

We examine in computer simulation and theory some important properties of the distributions of electrons heated by resonance absorption of intense laser light. Comparison is made with recent experiments.

Recent experiments[1,2] have shown that resonance absorption is an important process in the absorption of intense laser light. In this Letter we present some important features of resonantly heated electrons, including their Maxwellian character, and their dependences on laser light intensity and background plasma temperature. We begin with simulation results obtained with the same ideal model[3] previously used to establish the importance of density profile steepening and to provide estimates for the magnitude of the absorption and its polarization and angle dependence. These early results predicted the qualitative features of the experimentally measured absorption (polarization dependence and broad angular dependence) and were sufficient to predict the magnitude within a factor of $\lesssim 2$. According to a two-dimensional (2-D) particle simulation code with relativistic dynamics and electromagnetic fields, plane light waves are propagated from vacuum into a plasma slab. Heated electrons reflect from the plasma sheath which forms on the vacuum side and are reemitted with their initial thermal temperature from the higher density boundary. After the density profile nonlinearly steepens, we measured the heated electron distribution and energy and the self-consistent scale length at the critical density.

In order to focus on the electrons heated by resonance absorption, we carried out a large number of simulations with p-polarized light incident at an angle of 24 deg, which is approximately the optimum angle in the steepened density profile. Figure 1(a) shows a typical heated electron distribution which is well approximated by a two-temperature Maxwellian.[4] The lower energy particles simply represent the initial thermal distribution which streams in from the higher-density plasma, and the higher-energy Maxwellian represents the resonantly heated electrons with "temperature" $T_{\rm hot}$. This quasi-Maxwellian form of the heated electron distribution has been suggested by laser-plasma experiments,[5] where it is typically observed that the high-energy x rays decrease exponentially with energy. Maxwellian heated distributions have been directly observed in experiments with microwaves and have been attributed to electron heating by very localized fields.[6] Incidentally, we have also simulated examples of stimulated Brillouin backscatter that heats ions to a Maxwellian distribution.

The local density scale length near the critical density becomes quite steep. A crucial feature of the scale length (L) is its intensity dependence,[4] which is shown in Fig. 1(b). As the light intensity (I_L) increases, L decreases as $I_L^{-\beta}$, where

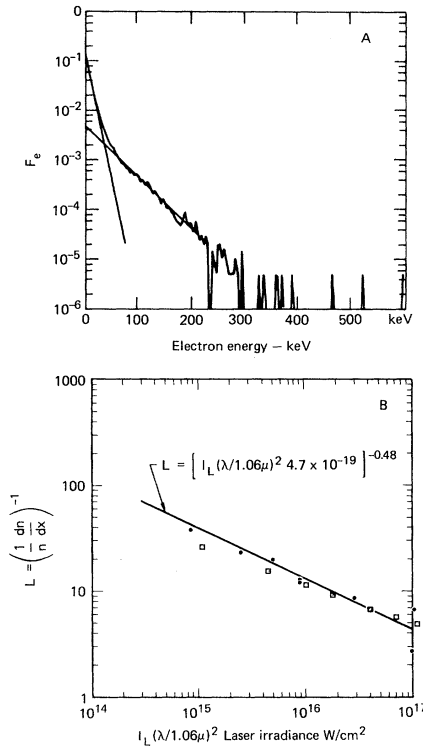

FIG. 1. (a) The electron distribution function, number vs energy, from a typical 2-D simulation. The parameters are $\omega_0 t = 367$, $v_L/c = 0.085$ (8.8×10^{15} W/cm^2 at $\lambda = 1.06$ μm), angle 24 deg, $T_e = 4$ keV, and $T_e/T_i = 3$. $T_{\rm hot}$ is defined as the hot slope of this distribution. (b) The steepened scale length in λ_D defined with the initial T_e and at the critical density vs the incident light intensity. The parameters are $T_e = 4$ keV, $T_e/T_i = 3$, and angle 24 deg. The boxes are the theoretical prediction.

$\beta \simeq 0.48 \pm 0.07$ in these simulations.

This intensity dependence of the steepened scale length is important, since this scale length indirectly controls the heated electron energies. In particular, the dependence of the heated electron energy becomes, in general, weaker than the square root dependence previously estimated.[7] This is confirmed by simulation results.[8,9] As shown in Fig. 2(a), the heated electron energy measured in our simulations scales as I_L^{β}, where $\beta \simeq 0.39 \pm 0.07$. The hot temperature here is defined as $\frac{2}{3}$ of the slope of the high-energy part of the 2-D electron distribution, e.g., Fig. 1(a). Note that these are 2-D simulations and that the heating primarily occurs in the direction of the density gradient. If the electrons are isotropized in angle at higher density [either by collisions with highly stripped (high-$\bar{z}$) ions or by magnetic fields due to the Weibel instability or other magnetic field sources] the temperature of the isotropized distribution is $\frac{2}{3}$ of the values from the 2-D simulations. Of course, the average hot-electron energy is the same in 2-D as the hot temperature, and in 3-D the average energy is 1.5 the temperature. Since L also depends on the background plasma temperature T_e, the heated electron energy will likewise depend on this temperature. As shown in Fig. 2(b), this dependence is fairly weak[9]: $T_{\rm hot} \propto T_e^{\gamma}$, where $\gamma \simeq 0.25 \pm 0.07$. An empirical formula that fits Fig. 2 reasonably well is $T_{\rm hot} = 1.2 \times 10^{-5} T_e^{0.25} \{I_L[\lambda/(1.06\ \mu\text{m})]^2\}^{0.39}$ for $T_e/T_i = 3$. Another formula that fits well is $T_{\rm hot} = T_e + 4.3 \times 10^{-6} T_e^{0.04} \{I_L[\lambda/(1.06\ \mu\text{m})]^2\}^{0.42}$. Both formulas give about the same answers in the parameter range of the simulations. However, they differ considerably at low T_e and/or low I_L where simulation is not economically feasible at this time. For high T_e/T_i, our two data points in Fig. 2(b) show a shorter scale length and lower $T_{\rm hot}$ presumably due to the lower ion pressure. Of course, the relevant parameter in the experiment is $\bar{z}T_e/T_i$. $T_{\rm hot}$ as a function of angle is shown in Fig. 3(a).

In the simulations, the fractional absorption (f) was nearly a constant at the different intensities; i.e., $f \simeq (47 \pm 10)\%$ (less with the initial density step condition). Most of the runs started off with a ramp profile in which the density initially varied linearly (from 0 to $1.7 n_{\rm cr}$ in three vacuum light wavelengths, or by a lower density shelf plus a steep gradient to a higher density shelf (see Ref. 3, Fig. 5). The higher intensity simulations were rerun with an initial sharp step profile with quasi pressure equilibrium and are shown by the open circles in Fig. 2(a). Pressure equilibrium was tested by starting with maximum density too high and letting it fall down and conversely by starting too low and letting the maximum density increase with similar $T_{\rm hot}$'s resulting. The temperatures with the initial step profile were initially colder, but gradually increased to approximately (but still lower than) the values obtained with the ramp profile as the lower density plateau established itself. $T_{\rm hot}$ increases rapidly with the shelf density because of pump swelling and longer-wavelength plasma waves driven in that lower density region [Fig. 3(b)]. Of course, the history of the laser pulse and hydrodynamic motion affect the density plateau.

We can gain insight into the physics via a very simple model. We adopt the capacitor model (an oscillating electric field $E_d \cos\omega_0 t$ applied to a plasma with a linear density gradient with a scale length L). The amplitude of the resonantly driv-

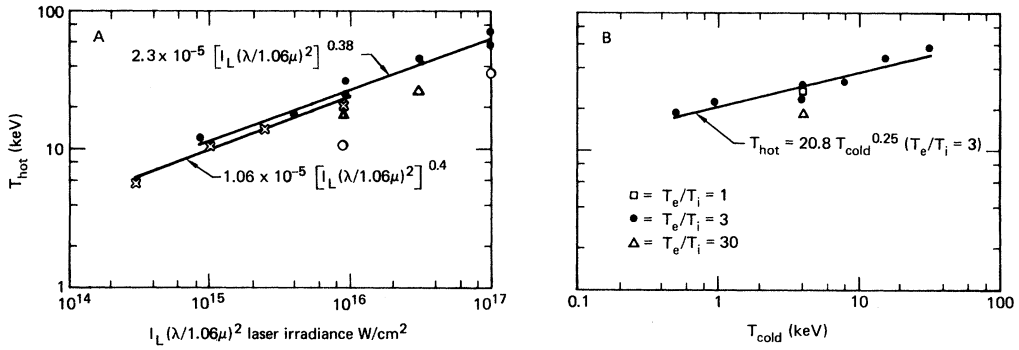

FIG. 2. (a) The heated electron temperature (assuming 3-D isotropization) vs the incident light intensity from a series of 2-D simulations. The angle is 24 deg. The crosses are for $T_e = 1$ keV, and the points are for $T_e = 4$ keV. The open circles are from simulations with an initial step profile with $T_e = 4$ keV at early times. (b) The heated electron temperature vs initial background plasma temperature from a series of simulations in which the angle is 24 deg, and $v_L/c = 0.085$.

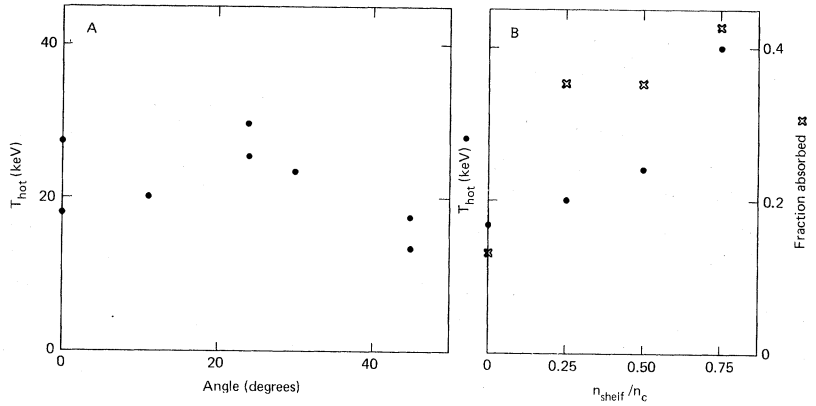

FIG. 3. (a) T_{hot} as a function of angle. $v_L/c = 0.085$, $T_e = 4$keV, $T_e/T_i = 3$. (b) T_{hot} and fraction of light absorbed vs lower shelf density with fixed ions. $v_L/c = 0.085$, $T_e = 4$ keV, $L = 11\,\lambda_{De}$.

en plasma field (E_w) and its spatial extent (l_{int}) can then be estimated in a warm-plasma, wave-breaking limit.[10] This gives

$$v_w = -1.5v_e + (2.25v_e^2 + 2\omega_0 L v_d)^{1/2} \quad (1)$$

and $l_{int} = 2(x_w + 3\lambda_{De})$, where v_e is the electron thermal velocity $(T_e/m_e)^{1/2}$, λ_{De} the electron Debye length, $V_w = eE_w/(m\omega_0)$, $x_w = v_w/\omega_0$, and $v_d = eE_d/(m\omega_0)$. Note that these expressions reduce to the cold-plasma wave-breaking ones[11] when the estimated thermal corrections are neglected.

In this simplest model we next estimate the steepened scale length by simply balancing the thermal pressure with the ponderomotive pressure of the localized plasma field; i.e., $T_e \partial n/\partial x = ne^2/(4m\omega_0^2)\partial E_w^2/\partial x$. Using $\partial E_w^2/\partial x \simeq E_w^2/(l_{int})$ then gives

$$L = 8(x_w + 3\lambda_{De})/(v_w/v_e)^2. \quad (2)$$

Lastly, to relate the capacitor model to the situation of p-polarized light incident onto a plasma, we balance the energy fluxes: $fcE_L^2/8\pi = \omega_0 L E_d^2/8$, where E_L is the free-space value of the electric vector of the light and c is the speed of light. Hence,

$$v_d = v_L(fc/\pi\omega_0 L)^{1/2}. \quad (3)$$

Equations (1)–(3) suffice to determine L and v_w in terms of the incident light intensity, the absorption efficiency, and the background temperature. The theoretical results for L are shown by the boxes in Fig. 1(b). Note that this very simple model is sufficient to capture the basic physical effect: L decreases as the intensity increases. Indeed, the predicted intensity dependence is nearly that observed in the simulations. This simple model seems to overestimate the temperature dependence of L. L is predicted to scale as T_e^{δ} where $\delta \approx 1$, whereas the simulations show a weaker dependence on L on temperature. This indicates that an improved model taking into account laser light pressure, heated electron pressure, and plasma flow is, in general, necessary.

We can readily understand the intensity dependence of T_{hot} in terms of the intensity dependence of L. Again appealing to the capacitor model, $T_{hot} \propto eE_d L$, or in terms of the light intensity, $T_{hot} \propto E_L L^{1/2}$. Hence, we expect $T_{hot} \propto I_L^{\beta}$, where $\beta \simeq 0.26$. This estimate is about 30% lower than the simulation results but is still in reasonable agreement.

Lastly, recent experimental results[12,13] indicate that the hot-electron temperature does scale less weakly than $\{I_L[\lambda/(1.06\ \mu\text{m})]^2\}^{1/2}$ over a wide intensity regime. Figure 4, which is taken from Ref. 12, shows T^* as a function of intensity measured in many different experiments with different target materials, where T^* is the "temperature" deduced from the slope of the high-energy x rays. T^* is a function of target material and for a given material (Parylene) varies as $I_L^{0.31}$ over a wide intensity regime from 10^{14} to 10^{17} W/cm^2 (1.06-μm light). This dependence is in reasonable agreement with that suggested by these ideal simulations. More importantly, this weaker intensity dependence holds even for modest intensities like 10^{14} W/cm^2. This consistent with our interpretation that the resonantly excited plasma waves locally steepen the density gradient, an effect which does not require a light pressure as large as the plasma pressure.

This correlation is encouraging, but a number of qualifications are in order. First, $T^* \neq T_{hot}$. LASNEX calculations[14] show that T^* is often significantly lower in magnitude (factor of ~2) than T_{hot} because of the space and time integrations inherent in the measurements and also the gen-

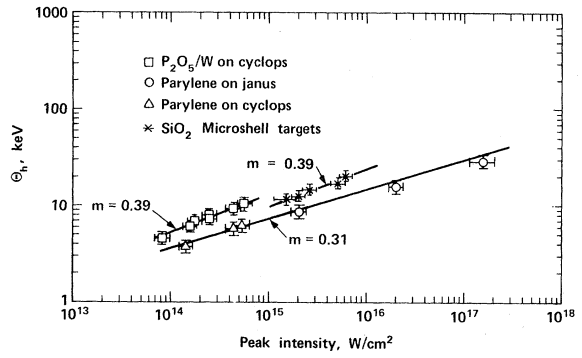

FIG. 4. The hot temperature, T^*, inferred from the high-energy x rays vs laser light intensity. Note also the dependence on target material. This figure is from Ref. 12.

eral features of the hot-electron transport. Secondly, we note that the values of T_{hot} inferred from Fig. 2(a) are typically 1.3 to 2 times T^* shown in Ref. 12. This is also to be expected, since in the ideal simulations we are considering the nearly optimum angle of incidence and also a higher background temperature than may be obtained in the experiments. Both our simulations and simple model show that T_{hot} is smaller for other than optimum angles of incidence (see Fig. 3) and also for smaller ion-electron temperature ratios. Although the simulations we have discussed illustrate the physics, improved models for more quantitative comparisons must allow for (1) a distribution of angles of incidence; (2) T_e/T_i and ionization states; (3) the admixture of other absorption processes; (4) more complex particle boundary conditions than the one-pass model discussed here; and (5) the lower shelf density. For example, the larger heated temperature for the higher-z targets is at least partly due to the fact that the heated electrons are more often reflected from the high density plasma back into the heating region. Simulations show about a 25% increase in temperature when the electrons make on the average two passes through the absorption regions.

We are happy to acknowledge valuable conversations with A. B. Langdon and R. A. Haas.

[1]K. R. Manes *et al.*, Phys. Rev. Lett. 39, 281 (1977).

[2]J. S. Pearlman, J. J. Thomson, and C. E. Max, Phys. Rev. Lett. 38, 1397 (1977); J. E. Balmer and T. P. Donaldson, Phys. Rev. Lett. 39, 1084 (1977); R. P. Godwin, P. Sachsenmaier, and R. Sigel, Phys. Rev. Lett. 39, 1198 (1977).

[3]Kent Estabrook, E. J. Valeo, and W. L. Kruer, Phys. Fluids 18, 1151 (1975), and Phys. Lett. 49A, 109 (1974).

[4]Kent Estabrook, Bull. Am. Phys. Soc. 21, 1067 (1976).

[5]B. H. Ripin *et al.*, Phys. Rev. Lett. 34, 1313 (1975); C. Yamanaka *et al.*, Phys. Rev. Lett. 32, 1038 (1974); J. F. Kephart, R. P. Godwin, and G. H. McCall, Appl. Phys. Lett. 25, 108 (1974); W. C. Mead *et al.*, Phys. Rev. Lett. 37, 489 (1976); P. Kolodner and E. Yablonovitch, Phys. Rev. Lett. 37, 1754 (1976).

[6]P. DeNeef and J. S. DeGroot, Phys. Fluids 20, 1074 (1977).

[7]J. Albritton and P. Koch, Phys. Fluids 18, 1139 (1975); J. P. Freidberg *et al.*, Phys. Rev. Lett. 28, 795 (1972); D. W. Forslund *et al.*, Phys. Rev. A 11, 679 (1975).

[8]E. Valeo *et al.*, in *Proceedings of the Sixth International Conference on Plasma Physics and Controlled Nuclear Fusion Research, Berchtesgaden, West Germany, 1976* (International Atomic Energy Agency, Vienna, 1977), pp. 133–146.

[9]D. W. Forslund, Bull. Am. Phys. Soc. 21, 1066 (1976); D. W. Forslund, J. M. Kindel, and K. Lee, Phys. Rev. Lett. 39, 284 (1977).

[10]W. L. Kruer, to be published.

[11]P. Koch and J. Albritton, Phys. Rev. Lett. 32, 1420 (1974).

[12]K. R. Manes *et al.*, J. Opt. Soc. Am. 67, 717 (1977).

[13]R. Spielman, K. Mizuno, and J. S. DeGroot, Bull. Am. Phys. Soc. 22, 1188 (1977).

[14]W. C. Mead, private communication.